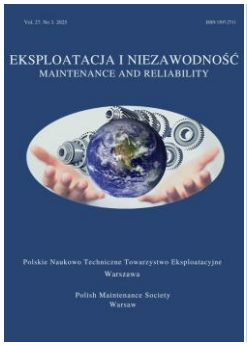

Eksploatacja i Niezawodnosc – Maintenance and Reliability
Volume 27 (2025), Issue 3
journal homepage: http://www.ein.org.pl

Article citation info:
Zhu L, Energy management in microgrid integrated with ultracapacitor-equipped electric vehicles and renewable resources using Hybrid Algorithm Perspective, Eksploatacja i Niezawodnosc – Maintenance and Reliability 2025: 27(3) http://doi.org/10.17531/ein/200713

Energy management in microgrid integrated with ultracapacitor-equipped electric vehicles and renewable resources using Hybrid Algorithm Perspective

Indexed by:
Web of Science Group

Lidong Zhu[a,*]

[a] Jilin Railway Technology College, Jilin City, China

Highlights

- New method for managing hybrid renewable energy in smart grids.
- Electric vehicles' role in expanding the electricity market.
- Optimize to boost electricity production and cut costs.

Abstract

A novel optimization method, based on the Big Bang-Big Crunch hybrid algorithm, is employed to manage the timing and integration of EVs into the microgrid, aiming to minimize operational costs. The algorithm efficiently controls the energy flow between the EV batteries and the control system, dynamically adjusting to meet demand while reducing costs. The system was tested on the IEEE 14-bus system with real EV movement patterns over a 24-hour period. The results show a significant cost reduction, with the total cost decreasing from $132,869.9 without EVs to $112,981 when EVs equipped with ultracapacitor batteries are integrated, representing a 15% reduction. Moreover, the proposed method outperforms other algorithms, such as Particle Swarm Optimization (PSO) and Genetic Algorithm (GA). Compared to these methods, the Big Bang-Big Crunch hybrid algorithm achieves cost reductions of 17% over PSO and 13% over GA, demonstrating its effectiveness in optimizing energy management in a microgrid with renewable energy sources.

Keywords
photovoltaic-wind hybrid systems, electric vehicles, Big Bang Big Crunch hybrid algorithm, accessibility.

1. Introduction

In traditional networks, supplying electric power required by the consumer is produced in a complex manner and far from the consumer, which has caused problems. From among these problems, we can refer to the high cost of building power plants and transmission lines at higher capacities, as well as the high losses of this type of networks [1]. Another defect of traditional networks is the low reliability of such networks, since if an error occurs and the transmission lines are cut, it is likely that many consumers will not have access to electricity [2]. Consequently, in order to overcome such problem, more and more attention has been paid to distributed production. Nowadays, using distributed generation method for electricity generation is one of the methods that has been recommended to supply the power required by the consumer [3-5]. Ref. [6] provides a detailed analysis of the real-time manifestation of islanding and islanding detection strategies (IDS). First, it focuses on presenting the concept of islanding detection, standardization of islanding detection, and an analysis of their advantages and disadvantages. Next, the detailed classification of the IDSS is presented with focus on remote and local methods. You can use passive, active and hybrids to classify local IDs. Microgrids are a collection of loads and producers that can work as islands or

(*) Corresponding author.
E-mail addresses: L. Zhu (ORCID: 0009-0000-7202-5766) zld19860920@163.com

connect to the grid. Producers of microgrids are distributed resource generators that include solar cells, wind turbines, microturbines, batteries, etc. [7]. However, power generation costs and environmental pollution caused by microgrids need to be addressed carefully [8-10]. Ref. [11] proposes a day-ahead scheduling system for a MG with solar power, focusing on the impact of weather on PV output. A modified fluid search optimization algorithm is used to improve energy management in grid-connected MGs with high unpredictability. Simulation results show enhanced energy management accuracy and reduced operational costs. Given the growing need for energy sources and the diminishing availability of fossil fuels, using renewable energy sources, such as solar and wind energy, can help maintain a clean environment and lower air pollution. With solar system installed capacity growing at a 60% annual growth rate, the use of renewable energies has expanded [12]. Despite having two significant drawbacks, namely the difficulty of accessing the generated electricity and the expensive cost of the equipment, DC systems are nonetheless more widely used than AC ones because of their higher levels of efficiency, dependability, and accessibility to renewable energy sources. To mitigate fluctuations in the production part of the hybrid system, a battery bank is used for energy storage, which absorbs excess power and provides power in various working conditions [13].

In [14], controlling strategy is presented with the aim of supplying the load of the system. The solar array is the main source of supplying power required by the system load in such a way that if only solar energy is available, the solar array alone can supply the system load. The excess power of the system is delivered to the electrolyzer for hydrogen production and to the battery for storage. In the photovoltaic-fuel cell mode, the solar array alone is not able to supply the load of the system; in this case, the fuel cell enters the circuit and contributes with the hydrogen stored in the tank in supplying the load with the solar cell. In this case, due to the uncertainty of solar radiation, it is not able to produce power; the system load is supplied only by the hydrogen stored in the tank and the power is produced by the solar cell.

A joint energy management and trading model for CCHP microgrids aims to reduce costs and improve efficiency by prioritizing self-generation and demand-side management is proposed in [15]. Microgrids can buy or sell energy to nearby grids or utilities when necessary, and diesel generators serve as backup when other energy sources are insufficient. This approach enhances system reliability and flexibility. In [16], deterministic algorithm method is used in order to determine the number and type of units optimally. Many researchers have proven that the direct algorithm is the most effective deterministic algorithm for finding the best solution in various problems. In the paper, the data of solar radiation intensity, wind speed and ambient temperature are recorded hour by hour for six months. The outcomes of simulation demonstrated that the separate hybrid solar/wind/diesel system with/without battery could be used as an economic technique for generating electric energy in remote areas, given its final costs. In [17], an optimal sizing method to optimize a hybrid photovoltaic-wind system with a battery, in which a genetic algorithm is used to optimize the size of the equipment according to the cost and reliability of the system. This paper assesses hybrid energy systems integrating PV, wind turbines, diesel generators, and storage options (fuel cells and batteries) for non-domestic loads in four locations in Cameroon. Using the Cuckoo Search Algorithm (CSA) for optimal sizing, the study finds that battery-based hybrid systems are more cost-effective than fuel cell systems in the short term. In [18], presents a hybrid energy storage system of battery fuel cell (FC) and passive control (PBC) for hybrid electric vehicles (HEVs) that improves power integration and increases operation speed. The first section describes the power management (PMC) that uses a fuzzy logic controller for the FC battery system to ensure continuous power supply. The second section describes the PBC method for vehicle permanent magnet synchronous motor (PMSM) considering nonlinearities and disturbances, and compares with proportional integral (PI) and sliding mode control (SMC) to evaluate the performance of PBC. Ref. [19] presents a microgrid integrating solar panels, wind turbines, a Li-ion battery system, an EV, and a DC load, connected through power converters to a DC bus and AC grid. The primary objectives include DC bus voltage regulation, optimizing renewable energy conversion, and maintaining energy quality. A novel energy management algorithm with fuzzy logic controllers, fine-tuned by Particle Swarm Optimization (PSO), enhances network stability and energy distribution. Simulations demonstrate significant improvements in control accuracy and system performance.

Previous research on energy management in EV integrated microgrids has focused primarily on managing EV charging and discharging based on charging curves and electricity prices. Although these approaches have several advantages, such as facilitating off-peak charging and selling stored energy to the grid during peak hours, they often overlook the potential of advanced storage technologies and optimization algorithms. Many of these studies rely solely on traditional rechargeable batteries for energy storage, which may result in limitations such as slow response times and high degradation rates during frequent charging cycles. Furthermore, the optimization techniques used in previous studies, such as traditional PSO and genetic algorithms (GA), may not be effective enough to minimize operational costs or maximize the efficiency of the system. The novelty of this paper lies in the integration of electric vehicles equipped with ultracapacitors into microgrids, combined with a smart optimization approach using a hybrid big bang-big crunch algorithm. Unlike traditional battery-based systems, ultracapacitors allow for faster discharge and recharge of energy, making them ideal for balancing the fluctuations of renewable energy sources such as wind and solar power. In this study, we present an integrated energy management model that optimizes the interaction between electric vehicles, renewable energy sources, and the power grid. Using the Big Bang-Big Crunch algorithm, we outperform PSO and GA, achieving significant cost savings and improved system performance. By incorporating real-world EV driving patterns and optimizing their grid integration timing, this study proposes a more dynamic and cost-effective solution for modern energy systems, addressing the limitations of previous approaches and advancing the field of intelligent microgrid energy management.

In Section 2, we discuss the structure of the proposed system, including the renewable energy sources and electric vehicles (EVs). Section 3 focuses on the optimization methods, specifically the Big Bang-Big Crunch hybrid algorithm used in the study. In Section 4, the results of the proposed method applied to the IEEE 14-bus system are presented. Finally, Section 5 concludes the paper by summarizing the key findings and contributions.

2. Modelling

In this paper, an advanced approach to energy management within microgrids, particularly focusing on the integration of electric vehicles (EVs) equipped with supercapacitor energy storage systems is investigated. this study considers a microgrid environment that incorporates renewable energy sources, specifically wind turbines and photovoltaic (PV) panels, which contribute to the system's energy supply. The presence of electric vehicles introduces unique challenges and opportunities for optimizing energy distribution and storage within the grid. To address these challenges, a comprehensive optimization algorithm based on the Big Bang method, aiming to minimize the overall cost function is proposed. This algorithm effectively manages the dynamic and stochastic nature of energy generation and consumption in the microgrid, ensuring efficient energy utilization and cost reduction while maintaining system stability. Our findings demonstrate that the proposed approach significantly enhances the performance and economic feasibility of microgrids with integrated EVs and renewable energy sources.

2.1. Vehicle to grid technology (V2G)

Currently, power grids have very limited storage systems and, for this reason, matching production, and consumption in them requires permanent management and control of electrical energy generating units. Based on the researches it is found that limited-range electric vehicles (EVs) can meet the daily driving needs of a large proportion of drivers, with 9% of drivers never driving more than 100 miles per day and up to 32% of drivers willing to adapt their needs. driving speed several times a day. Furthermore, at least 75% of vehicles are always parked, indicating that the impact of EV charging on the grid is manageable, the batteries of these cars can provide a powerful storage system with high availability for the power grid [20]. In this way, an unused capital can act as an active element in the network and provide the energy stored in its battery to the network. What attracts the attention of so many people and researchers to electric vehicles is the concept of vehicle to network technology (V2G).

V2G concept is initially associated with two large and independent systems, including the power generation system and the transportation system. This concept is completed through two-way connection between these two systems in the smart network environment. To put it another way, V2G means

that electric vehicles can transfer power from the grid to the cars during charging and transfer power from the cars to the grid when the cars are used as storage which is shown in Fig.1.

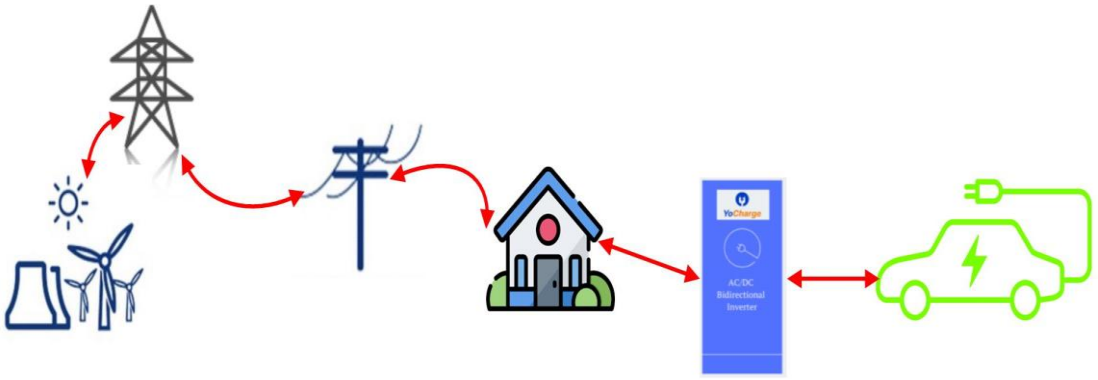

Fig. 1. V2G structure.

After the introduction of electric and hybrid vehicles, which are only able to receive electricity from the network, a conventional design for electric vehicles is proposed by making simple changes in the power circuits of these cars. Hence, they can connect to the V2G network, in such a way that enabled them to transfer the energy stored in their batteries to the network when the vehicle is parked [21]. So, V2G can have a two-way exchange with the network, creating many opportunities that increase efficiency and reliability [22]. The electrical network must gather information to create two-way transfer of power and power-related data between network components and consumers, which requires the establishment of charging and discharging infrastructures. The result of this complexity in the transfer of data and energy is the need to expand the standards of each part of the valuable V2G chain. These standards include physical infrastructure alongside virtual standards that include communication, data security, convenience, and information transfer among stakeholders [23].

One of the most important infrastructures required for the V2G system is fast charging and discharging stations for machines, requiring the use of new technologies for their production. These stations should have the ability of two-way connection to the network and should be designed and built according to the requirements and standards of operating companies in the field of electrification. Another category of infrastructure is related to the communication and measurement requirements of the smart network. In order to initiate V2G with all the functions and benefits that are discussed before, we need a smart network to manage and control the charging and discharging of cars. Initiating the smart grid itself requires smart measurements and telecommunication systems. Telecommunication systems in smart network can be formed in two ways, considering the electric vehicles: PLC and wireless.

When EVs are parked, they are considered an unused capital and it is not even possible to impose costs such as parking fees, etc. V2G is a concept that is designed to utilize this unused capital. Each V2G has a converter and a battery, and the structure of each V2G can be considered as shown in Fig.2.

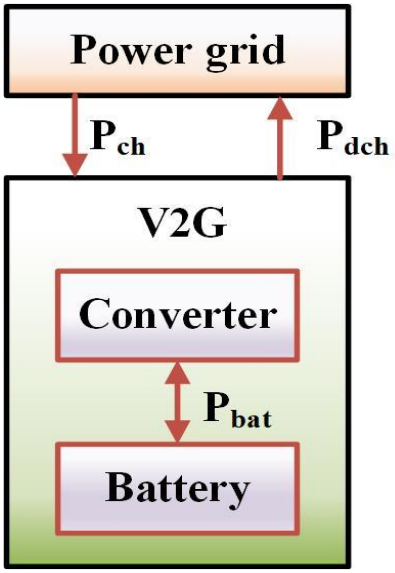

Fig. 2. The internal structure of V2G.

The power of V2G exchange with the network is defined as follows:

$$P_{ch} = \frac{P_{bat}}{\eta_c} \quad (1)$$

$$P_{dch} = P_{bat}\eta_d \quad (2)$$

P_{Bat} is the amount of power that V2G can transfer to or receive from the converter. It charges the battery with the efficiency of η_c and delivers battery power to the network with the efficiency of η_d. Eq.1 and Eq.2 indicates that if η_c and η_d are not the same unit, V2G must buy more power than it stores to

charge its own battery, while the power it delivers to the network is less than the power stored in the battery. Therefore, the closer η_c and η_d are to one, the more profit V2G owner gets from using its battery capacity [23].

2.2. Solar energy and photovoltaic

Solar energy can be used in various ways, the most common of which is providing hot water for homes. A simple method is to transfer solar energy to a boiler by means of reflectors and use the created steam to turn a steam turbine. Another method is to convert solar energy directly into electricity using photovoltaic cells. In this method, the efficiency is about 30% to 37%. Currently, due to the high price of photovoltaic cells, it is an expensive design. However, it is hoped that more research is done in this field and the costs are reduced [24]. Photovoltaic (PV) systems are an important component of renewable energy production, converting sunlight directly into electrical energy through solar cells made of semiconductor materials such as silicon. When sunlight hits a photovoltaic cell, it excites electrons and creates an electric field that produces direct current (DC), which is then converted to alternating current (AC) for use in homes and businesses. This technology forms the basis of solar energy and is critical to driving sustainable energy solutions for a variety of applications, from small residential installations to large solar power plants.

2.2.1 Output power of PV

Photovoltaic systems are increasingly used in microgrids to provide reliable, clean energy, reduce dependence on fossil fuels, and increase energy sustainability. Microgrids often integrate photovoltaic systems with energy storage solutions, allowing excess energy produced during peak hours to be stored and used during times of less sunlight or higher demand. It not only stabilizes the microgrid, but also optimizes energy efficiency, making it a key solution for remote or off-grid areas and contributing to global sustainability [24].

The output power P_{pv} of a photovoltaic module can be calculated using the following formula:

$$P_{PV} = \eta \times A \times G \times (1 - T_C) \quad (1)$$

Where,

η is the efficiency of PV module, and A is the area of the PV module (in square meters). G is the solar irradiance incident on the PV module (W/ m^2). TC is the temperature coefficient, representing the loss of efficiency due to temperature increases above the standard test conditions (STC) temperature, typically 25°C.

2.3. Wind energy

Wind turbines are an important part of renewable energy systems that use the kinetic energy of the wind to generate electricity. These turbines consist of large blades mounted on a rotor that spins as the wind blows. The rotary motion drives a generator, which converts mechanical energy into electrical energy. Wind turbines are usually installed in wind farms on land or offshore, and together they produce large amounts of electricity. This technology is key to reducing greenhouse gas emissions and various energy excellence, which promotes a more sustainable and flexible energy infrastructure. Microgrid wind turbines are often used with other renewable energy sources, such as photoelectric (PV) systems to provide a stable and continuous power supply. The integration of micro -grid medium wind turbines has enhanced energy reliability, especially in areas with the same wind mode. The generated power can be directly used or stored in the battery for future use during low winds. This not only optimizes the use of renewable resources, but also reduces dependence on fossil fuels, making microgrids an efficient and environmentally friendly solution for urban and remote areas [25].

2.3.1. Output power of WT

The actual power is also extremely dependent on the wind speed, as the power available from the wind is proportional to the cube of the wind speed.

When considering a wind turbine's power output, consider the cut-in speed (v_{cut-in}) and the cut-out speed ($v_{cut\text{-}off}$) model is critical. Wind turbine output power P as a function of wind speed v can be expressed as follows:

$$P_{wt}(v) = \begin{cases} 0 if\, v < v_{cut-in} \\ P_{rated} \times \left(\frac{v^3 - v_{cut-in}^3}{v_{rated}^3 - v_{cut-in}^3}\right) if\, v < v_{cut-in} < v_{rated} \\ P_{rated} if\, v_{rated} < v_{cut-in} < v_{rated} \\ 0 if\, v > v_{cut-out} \end{cases} \quad (2)$$

Where:

$P_{wt}(v)$ is the power output at a given wind speed v. v_{cut-in} is the cut-in wind speed, the minimum wind speed at which the turbine begins generating power. $v_{cut-out}$ is the cut-out wind

speed, the maximum wind speed at which the turbine stops operating to avoid damage. v_{rated} is the rated wind speed, the wind speed at which the turbine generates its maximum (rated) power output. P_{rated} is the rated power output of the turbine at the rated wind speed.

This formula reflects that the turbine does not produce power at very low wind speeds, also stops generating power at very high wind speeds to protect the turbine from potential damage. Between the cut-in and rated wind speeds, the power output increases with the cube of the wind speed, reflecting the increasing kinetic energy available in the wind. Once the wind speed reaches the rated value, the turbine continues to produce its maximum power output P_{rated} until the cut-out speed is reached.

This model is crucial for understanding and predicting the performance of wind turbines in various wind conditions, particularly when integrating wind energy into microgrids where stable and predictable power output is essential.

2.4. Hybrid energy storage system and method

There are several ways to generate electricity, and one of them is through the use of storage devices. These devices convert chemical energy into electrical energy through chemical reactions. Hybrid energy storage systems (HESS) and battery systems are the most commonly used storage devices in the electric vehicle industry. However, they face challenges such as limited life cycle due to sink current, temperature changes, and restricted power density resulting in larger size and weight. An electric vehicle's energy storage system (ESS) must have wider characteristics than a simple battery since it needs to provide enough energy for long distances at a steady state, good acceleration, and transient rating powers. To address these challenges, a main ESS can be hybridized with a secondary ESS to protect the battery from high flow pressure. Flywheel energy storage system (FESS), ultracapacitors (UC), and superconducting magnetic energy storage (SMES) are proposed ESSs for EV applications. UC-battery hybrid systems are the most promising HESSs in recent studies due to their long-life cycle, quick response time, quick charging time, high efficiency, and low maintenance. Fig. 3 depicts the UC-HESS battery used in our proposed electric vehicles with Battery with UC in mode can be used to generate braking power [26].

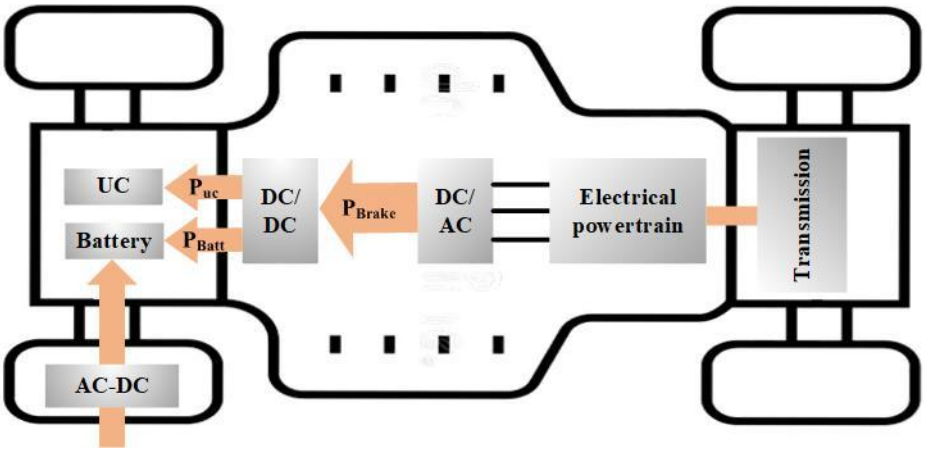

Fig. 3. hybrid charging of HESs in Evs.

The power output P_{UC} of an ultracapacitor in the electric EVs formulated by using the following formula:

$$P_{uc} = \frac{V_{uc}^2}{4R_{uc}} \quad (3)$$

Where:

-P_{uc} is the power output of the ultracapacitor (W).

- V_{uc} is the voltage across the ultracapacitor (V).

- R_{uc} is the equivalent series resistance (ESR) of the ultracapacitor (Ω).

This formula accepts that the ultracapacitor is being discharged optimally. The power delivered by the ultracapacitor be contingent on its voltage and internal resistance.

Alternatively, the energy stored E in an ultracapacitor, which influences the power output, is given by:

$$E = \frac{1}{2} C V_{uc}^2 \quad (4)$$

Where:

-E is the energy stored in the ultracapacitor (J).

- C is the capacitance of the ultracapacitor (F).

-V_{uc} is the voltage across the ultracapacitor (V).

The power output is a function of how quickly this stored energy can be released, which is directly related to the capacitance, the voltage, and the internal resistance of the ultracapacitor. This makes ultracapacitors particularly effective in applications requiring quick bursts of energy, such as acceleration in electric vehicles.

3. Modeling the problem of power generation and storage management

In this paper, we develop an energy management strategy for a microgrid integrating renewable energy sources, such as wind turbines and photovoltaic (PV) systems, and electric vehicles connected to a hybrid energy storage system (HESS) consisting of batteries and ultracapacitors. The main objective is to minimize the operational costs of the microgrid while ensuring a stable and reliable power supply. The energy management process is designed in such a way that the DC bus is mainly powered by electricity generated from wind and solar resources. When renewable generation is insufficient, energy is taken from the battery. If additional power is still required, a certain amount of electricity will be purchased from the grid, but this option is considered a last resort. This structured approach minimizes grid power consumption, thereby reducing costs and maximizing the efficiency of the use of renewable energy in the microgrid. The renewable energy management problem is considered as a mixed-integer nonlinear programming problem. The operational cost of the microgrid, which includes renewable resources, storage systems, and electric vehicles, is discussed in the subsequent section.

3.1. Costs

Most of the system costs contain the price of PV panels, WT, HESS and EVs. The total cost of the MG (dollars per year) contains initial costs and operation and maintenance costs, which can be expressed as the following formula:

$$Cost = C_{Grid} + \frac{\sum_{i=PV,WT,HESS}(I_i + OM_i)}{N} + \sum_{v=1}^{N_v} P_{EV}(v,t)\Omega(t) \quad (5)$$

where I_i and OM_i stand for each element's initial purchase price and ongoing operating and maintenance costs, respectively. N, C_{Grid}, and Cost stand for the system's life cycle, the cost of grid power input, and the system's overall annual cost in dollars. N_v is the number of EVs and $P_{EV}(v,t)$ is the amount of EVs power in time t. if the EVs is in the charging mode the injected power to grid is as load and if the EVs is in the discharging mode the injected power isas a battery with negative amount. Hence, the first objective function is formulated as follows:

$$\text{Min: } \{Cost(A_{PV}, A_{WT}, P_{HESS}, \psi)\} \quad (6)$$

A_{PV}, A_{WT}, P_{HESS} and ψ are the parameters designed in this paper, which respectively express the panel surface area, the footprint area, the HESS capacity, and the input power ratio from the network to the load.

The initial and operation and maintenance costs for the photovoltaic subsystem are expressed as follows:

$$I_{PV} = \lambda_{Pv} A_{PV} \quad (7)$$

$$OM_{PV} = OM_{yearly} A_{PV} \sum_{i=1}^{N} \left(\frac{1+v}{1+\gamma}\right)^i \quad (8)$$

where OM_{yearly}, v, and γ depict the annual operating as well as cost of maintenance in each unit, amplification rate and the rate of interest, respectively. Besides, I_{PV} and OM_{PV} are the initial cost and the total cost of operating and maintaining the solar subsystem, respectively. λ_{PV} also shows the cost of the panel, which is 525 \$/m^2.

The initial and operating as well as cost of maintenance for the wind turbine subsystem are similarly expressed by:

$$I_{WT} = \lambda_{WT} A_{WT} \quad (9)$$

$$OM_{WT} = OM_{yearly} A_{WT} \sum_{i=1}^{N} \left(\frac{1+v}{1+\gamma}\right)^i \quad (10)$$

where, I_{WT}, OM_{yearly} and OM_{wind} respectively show the initial cost, the annual operation as well as cost of maintenance in each unit and the total cost of operation and maintenance of the wind subsystem. Also, λ_{WT} represents the cost of the wind turbine which 100 dollars per square meter (\$/m^2).

The initial and operating as well as cost of maintenance for the battery bank are formulated by:

$$I_{HESS} = \lambda_{HESS} A_{HESS} \quad (11)$$

$$OM_{HESS} = OM_{yearly} P_{HESS} \sum_{i=1}^{T_b} \left(\frac{1+v}{1+\beta}\right)^{(i-1)N_{HESS}} \quad (12)$$

where I_{HESS}, OM_{yearly}, OM_{HESS} and β, respectively, represent the initial cost, the annual operation as well as cost of maintenance in each unit, the cost of operation and maintenance of the battery subsystem and the inflation rate. Moreover, λ_{HESS}, which represents the cost of the battery bank, is 100 dollars per kilowatt hour.

The HESS has a shorter lifespan compared to solar cells and

wind turbines, which means that they need to be replaced multiple times throughout the system's lifespan. Therefore, the cost of operation and maintenance in Eq. (12) refers to the cost of replacing the HESS.

The cost of input power from the network is formulated as follows:

$$C_{Grid} = \sum_{i+1}^{T} P_{Grid,t}\lambda_{Grid} \quad (13)$$

where $P_{Grid,t}$ represents the power purchased from the grid in each unit and λ_{grid} represents the price of input power from the network, which is \$0.1 per kilowatt hour.

3.2. Accessibility

When energy is available, accessibility is obtainable as a significant pointer for the system. There is great variance among availability and reliability. Reliability is the system's capacity to function without failure, whereas accessibility is its capacity to supply electricity to the load. For instance, an extremely reliable PV system, in which mechanisms do not fail can have little access, if there is sufficient energy storage to provide the required load power during the night or on a cloudy day [27].

A certain level of accessibility can be achieved with many system settings. Accessibility for the considered time period is formulated as follows:

$$A = 1 - \frac{DNM}{D} \quad (14)$$

DNM is formulated as follow:

$$DNM = \sum_{t=}^{T\Sigma}[PHESS.SOC_{PV\,WT\,Grid\,D\,HESS,min} \quad (15)$$

where if the supplied power is bigger than or equal to the demand, u(t) is a zero-step function; if the demand is not encountered, it is supposed to be one.

A, DNM, $P_{HESS,min}$ (t), $P_{HESS,SOC}$ (t) and P_D(t) parameters are respectively the availability index, unmet demand (kWh per year), minimum charge of the battery bank at the time, charging status of the battery bank at the time and the amount of demand per unit of time.

The input power from the network is:

$$P_{Grid} = \psi(P_D(t) - P_{PV}(t) - P_{WT}(t) - P_{HESS}(t)) \quad (16)$$

$$P_{WT} = P_{WT}A_{WT}\eta_{WT} \quad (17)$$

$$P_{PV} = InsolationA_{PV}\eta_{PV} \quad (18)$$

In Equations (16) to (18), the parameters of P_{PV}, η_{pv}, Insolation, P_{wt} and η_{wt} respectively indicate the production power of the solar subsystem, efficiency of the PV, amount of sunshine to the superficial of the cell, production power of the WT and effectiveness of the wind turbine. Besides, P_{WT} indicating the power rating of the wind turbine generator is 5 kW.

Therefore, the second objective function can be stated as follows:

$$MaximizeA(A_{PV}, A_{WT}, P_{HESS}, P_{EVs}, \psi) \quad (19)$$

As mentioned in Equation (8), the operating life of the battery is shorter than the life of solar cells and wind turbines, so it is necessary to replace the batteries several times in a 20-year period.

The values of the hybrid system parameters are mentioned in Table 1.

Table 1. Parameter of hybrid system.

Parameter	Value
Life cycle of system (N)	20 years
Life cycle of HESS (N_{HESS})	5 years
Inflation rate(β)	8%
Efficiency rate(γ)	12%
Resonance rate(ν)	12%

Other limitations related to the system are listed in Table 2.

Table 2. parameter of renewable energy sources.

Parameter	Value
Minimum area of PV (A_{PVmin})	0
Maximum area of PV (A_{PVmax})	4221m^2
Minimum area of WT (A_{WTmin})	100m^2
Maximum area of WT (A_{wtmax})	4350 m^2

3.3. Limitations of the problem

3.3.1. Balance load

The amount of produced power and demand power should be balance on a period which is calculated as follow:

$$P_{Grid}(t) + P_{WT}(t) + P_{PV}(t) + \sum_{ev=1}^{N_{ev}} P_{EV}^{disch}(v,t) = \sum_{ev=1}^{N_{ev}} P_{EV}^{ch}(v,t) + D_t \forall t \in \{1,\dots,T\}/\forall v \in \{1,\dots,N_{EV}\} \quad (20)$$

3.3.2. The production capacity of active power

Output power of WT and PV ranges are between the minimum and maximum defined production power. Also, the power of the main network does not exceed the defined minimum and maximum values, every hour.

$$Pwt_{wt,max_{wt,min}} \quad (21)$$

$$PPV_{PV,max_{PV,min}} \quad (22)$$

$$PGrid_{Grid,max_{Grid,min}} \quad (23)$$

$P_{WT,min}$, $P_{PV,min}$ and $P_{grid,min}$ represent the minimum active power of PV, WT and grid at time t, respectively. Also, $PWT_{,max}$, $P_{PV,max}$ and $P_{grid,max}$ are the maximum active power of PV, WT and grid at time t, respectively.

3.3.3. Regulations related to electric vehicles

Electric vehicle batteries are not charged and discharged in the same time period.

$$X(v,t) + Y(v,t) \leq 1 \forall t \in \{1,\dots,T\}, X, Y \in \{0,1\} \forall v \in \{1,\dots,N_v\} \quad (24)$$

Where, X (v, t) and Y (v, t) is a binary variable and represent the charging and discharging mode of EVs.

Each electric vehicle's battery needs to be in energy balance. In the charge mode, $E_{trip}^{v,t}$is the last energy the EVs battery has before moving during time period t. EVs (V, T) is the energy stored in the vehicle battery up until the end of time period t.

$$E_S(v,t) = E_S(v,t-1) + \eta_{ev}^{ch} P_{EV}^{ch}(v,t) - E_{trip}^{v,t} - \frac{1}{\eta_{ev}^{disch}} P_{EV}^{disch}(v,t) \forall t \in \{1,\dots,T\}, X, Y \in \{0,1\} \forall v \in \{1,\dots,N_v\} \quad (25)$$

$\eta_{ev}^{ch}$and $\eta_{ev}^{disch}$are the charging and discharging efficiency for the EVs, respectively. During charging and discharging, we have losses, equal to the defined amount. The charging and discharging range for each electric vehicle according to the charging and discharging rate of the battery is as follows:

$$P_{EV}^{ch}(v,t) \leq P_{max,EV}^{ch} X(v,t)$$
$$P_{EV}^{disch}(v,t) \leq P_{max,EV}^{disch} Y(v,t) \forall t \in \{1,\dots,T\}, X, Y \in \{0,1\} \forall v \in \{1,\dots,N_v\} \quad (26)$$

$P_{max,EV}^{ch}$ and $P_{max,EV}^{disch}$ are the maximum charging and discharging power of the v-th electric vehicle.

So, to prevent damage to the battery of electric vehicles, it is possible to discharge up to the minimum level of ψ_v^{min} and charge up to the maximum level of ψ_v^{max}.

$$E_s(v,t) \leq \Psi_v^{max}$$
$$E_s(v,t) \leq \Psi_v^{min} \quad (27)$$

Ψ_v^{max} and Ψ_v^{min} depend on the range of battery capacity for each electric vehicle and are calculated according to the following equation:

$$\Psi_v^{min_v^{min_{Bat,EV}^{max}}} \Psi_v^{max_{Bat,EV}^{max}} \quad (28)$$

$E_{Bat,EV}^{max}$ is the maximum battery capacity of an electric vehicle. Φ_v^{max} and Φ_v^{min} are maximum and minimum battery capacity (%), respectively. The amount of energy stored in the battery of electric vehicles during the last period of connection to the grid before moving should provide the energy required for moving.

$$E_s(v, t_{last}^q) \geq E_{trip}^{v,t} \quad (29)$$

t_{last}^q indicates the last time when the electric vehicle is connected to the network and before starting the q-th time travel.

3.4. Optimization

3.4.1. Hybrid Big Bang-Big Crunch algorithm

The BC-BB algorithm is based on the concept of the big bang and big crunch in the universe, representing the creation and collapse of the universe. This algorithm is similar to other evolutionary algorithms, and it has two stages for generating the initial population [28]. The first stage is the Big Bang phase, where the population is randomly and uniformly distributed throughout the search space. Then comes the Big Crunch phase, which is a converging operator that produces a single output known as the center of mass. This center of mass is calculated using the following equation:

$$X_i^k = \frac{\sum_{j=1}^{N} \frac{X_i^{k,j}}{f_j}}{\sum_{j=1}^{N} \frac{1}{f_j}}, i = 1,2,\dots c \quad (30)$$

where X_i^k, is the i-th component from the center of gravity in the k-th iteration, and $X_i^{k,j}$ is the i-th component of the j-th Particle produced in the kth iteration. The value of the objective function of j and n points are the number of points or Particles and c is the number of control variables.

However, in the suggested HBB-BC method, the search capability of the BB-BC algorithm is increased by utilizing the capabilities of the PSO, which prevents from getting caught in the local optimal locations. Similar to the PSO method, the

HBB-BC algorithm uses general optimum points to create new points while local optimal points are employed to locate the centers.

$$X_i^{(k+1,j)} = \alpha_2 X_i^k + (1+\alpha_2)\left(\alpha_3 X_i^{gbest(k)}\right) + (1-\alpha_3)\left(X_i^{pbest(k,j)}\right) + \frac{r_j \alpha_z (X_{i\,max} - X_{i\,min})}{k+1} \quad (31)$$

In Eq. (31), $X_i^{pbest(k,j)}$ is the best location of the j-th Particle up to the kth iteration and $X_i^{gbest(k)}$ is the best general location up to the k-th iteration. In the proposed algorithm, α_2 and α_3 control the influence of the global best $X_i^{gbest(k)}$ and local best $X_i^{pbest(k,j)}$ positions on applicant updates.

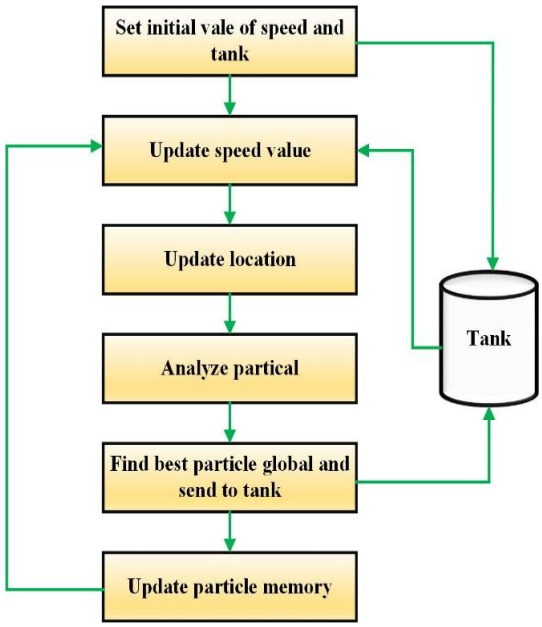

Fig. 4. Flowchart of HBB-BC algorithm [28].

Specifically, α_2 pulls applicants more strongly towards the global best, endorsing faster convergence towards a potentially optimal solution. In contrast, α_3 emphasizes adjustments around the local best, promotion examination within the applicant's neighborhood and helping avoid local optimal by indorsing diversity. Together, these parameters manage each applicant's position update each iteration, effectively balancing examination and exploitation. By doing so, they create a dynamic search behavior, where larger adjustments drive examination and smaller ones let for advanced searching in promising areas, enhancing the algorithm's ability to converge efficiently and robustly.The flowchart of HBB- BC algorithm is shown in Fig.4.

The order of implementing this algorithm is as follows:

1) Determining the required parameters for implementing the multi-objective Particle swarm algorithm, including the maximum repetition to implement the population size algorithm of α_2 and α_3 values and the amount of reservoir members.

2) The first population is established.

3) Each Particle's best individual response is chosen.

4) Separated non-dominant members are kept in the reservoir.

5) Each Particle selects a leader from the reservoir's members and executes its movement (updating its speed and position).

6) Each Particle's top individual response is updated.

7) The tank gains new recruits that are unstoppable.

8) The tank is empty of the victorious participants.

Now, by taking the variables into account, the multi-objective optimization algorithm calculates G_{best} throughout the whole population by considering a value for the error rate as Error while optimizing the values of the gains. Therefore, the cost function can be minimized by specifying the adjustment parameters of the above-mentioned algorithm.

4. Simulation result:

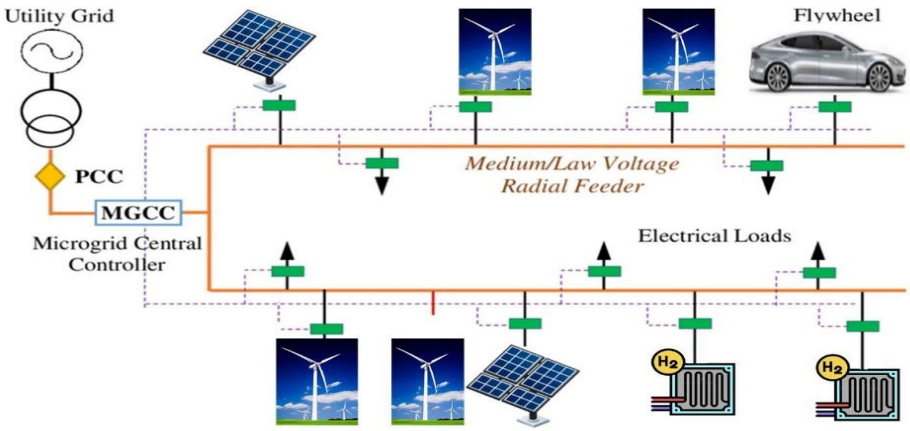

Fig. 5. Proposed MG structure.

The studied micro grid is shown in Fig. 5. This micro grid includes the main grid and ten scattered productions, including two PV with the capacity of 7 MW, two fuel cells (PAFC) with the capacity of 2MW, four WT with the capacity of 5 MW and, the electric vehicles which provide the energy needed by consumers.

In Fig. 6, the load curve and electrical price can be seen. According to the load curve, the peak consumption is 6785 kW. In this network, the price of electricity is not the same in different hours. Electricity is cheap in off-peak hours, but expensive in peak hours. Using multi-rate electricity prices is encouraged by the consumers and producers to reduce consumption during peak hours and increase production.

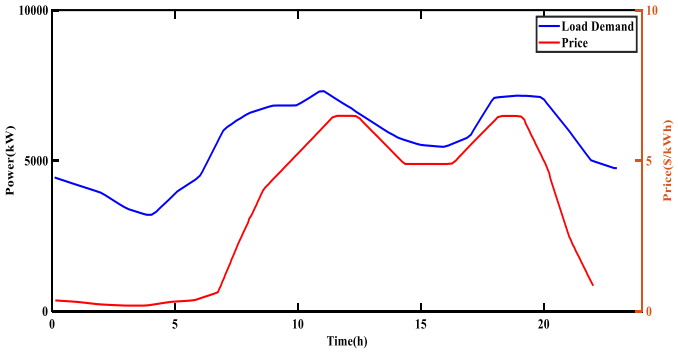

Fig. 6. Electrical load and price of energy curve of proposed MG.

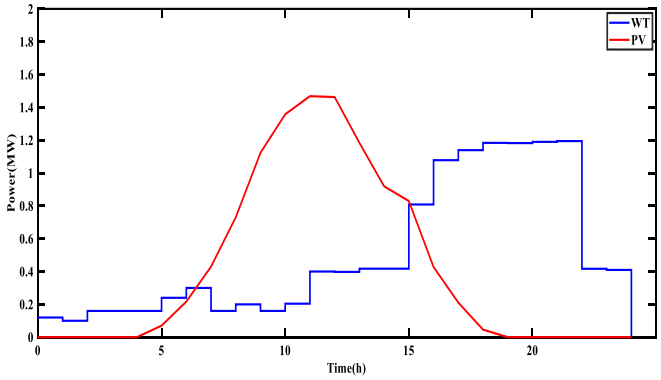

Fig. 7. produced power of WT and PV.

WT and PV systems cannot produce a constant amount of power in all hours of the day and night. Fig.7 shows the WT and PV power generation curve. In this network, 300 electric vehicles are used, which are divided into five groups based on the same conditions of the car owners. In the simulation, the connection of EVs to the network is considered as one, the absence of EVs in the network with the purpose of movement is considered as zero and the number two is considered for the standby mode. Standby is a mode in which EVs connected to the network are not studied and they are not moving either (does not participate in charging and discharging). Table 3 shows the presence and absence of EVs in the network.

Table 3. Presence or absence of EVs in MG.

Time	EV1	EV2	EV3	EV4	EV5
1	1	1	1	2	1
2	1	1	1	2	1
3	1	1	1	2	1
4	1	1	1	2	1
5	1	1	1	2	1
6	1	1	1	0	1
7	0	0	0	0	1
8	1	1	2	1	1
9	1	1	2	1	0
10	1	1	2	1	0
11	1	1	2	1	0
12	1	1	2	1	1
13	1	2	1	1	1
Time	**EV1**	**EV2**	**EV3**	**EV4**	**EV5**
14	1	2	1	1	1
15	1	2	1	1	1
16	1	2	1	1	1
17	0	2	1	1	1
18	0	1	0	1	1
19	0	1	0	2	0
20	1	0	1	2	0
21	1	0	1	2	0
22	1	1	1	2	1
23	1	1	1	2	1
24	1	1	1	2	1

In this paper, the simulation is done for 500 iterations, but in some cases, in order to comprehensive the simulation operation, the operation is repeated until that at least one of the following events happens as a termination condition:

HBB–BC: population size (N) = 500, $\alpha_1 = 1$, $\alpha_2 = 0.41$, $\alpha_3 = 0.82$, $P_m = 0.01$, maximum iteration = 500.

A) The algorithm spreads the maximum number of iteration (N=500).

b) The speed methods zero and the optimal answer is found.

Given the information about the number of electric vehicles and the time of connection to the network, it is assumed in the present study that the owners of electric vehicles move at constant speed and each EVs consumes an average of 3 kW power per hour. A point which should be mentioned when examining smart networks despite EVs are the energy stored in the EV's battery to cover the travel distance, which should be

sufficient. In this paper, we studied the Nissan car with a capacity of 24 kW and used the specifications of these EVs.

For scattered productions and different groups of electric vehicles, the maximum and minimum ranges of power alterations per hour are mentioned in Table 4.

Table 4. Max and min value of DG and EVS (kW)

Parameter	Min (kW)	Max (kW)
PAFC	200	2000
WT	0	5000
PV	0	7000
EV1(Tesla X plaid)	-760	760
EV2 (Porsche Taycan Turbo GT)	-815	815
EV3 (Audi SQ7)	-373	373
EV4(Nissan leaf)	-110	110
EV5(Bentley V8)	-467	467
Upstream grid	-15000	15000

The range of changes in charging and discharging power of electric vehicles per hour is selected according to the number of EVs in each category.

Table. 5 provides an overview of the power output functions for ultracapacitor in different EV. It highlights five EV models from different brands, including Tesla (Maxwell), UCAP Power, Audi E-Tron, Nissan Leaf and BMW i3. The table lists the minimum and maximum power for each model, starting from 5 kW in low-demand scenarios up to 300 kW for high-performance applications. These vehicle ultracapacitors range in capacity from 600 farads to 3400 farads depending on the specific needs of the vehicle. The supercapacitors in these models support quick bursts of power, especially during acceleration and regenerative braking, supplementing the battery system and improving overall efficiency and performance. These vehicles benefit from the fast charging and discharging capabilities of supercapacitors, making them ideal for meeting peak power requirements. To increase the battery life, when discharging EVs, it is better to leave at least 15% of the battery charge. The amount of battery charge should not be more than 90% of the EVs capacity. Hence, it should be checked every hour. If the EVs are power suppliers, the power of each group of EVs should not be less than the minimum defined in Table 5, after delivering power every hour. However, if they are consumers, the amount of power absorbed by each group of cars should not exceed the maximum limit defined in Table 5, after absorbing power every hour.

Table 5. Max and min capacity of battery.

EV Model	Brand	Min Power Output (kWh)	Max Power Output (kWh)	Ultracapacitor Capacity (F)
EV 1	**Tesla Model X plaid**	10	300	600 F - 3400 F
EV 2	**Porsche Taycan Turbo GT**	10	320	3000 F
EV 3	**Audi SQ7**	15	95	500 F - 3000 F
EV 4	**Nissan Leaf**	5	40	3400 F
EV 5	**Bentley V8**	10	300	3000 F - 3400 F

The ultracapacitors recorded in Table 5 play a crucial role in improving the energy management abilities of each EV model. With their high-power density, ultracapacitors can quickly save and release energy, allowing EVs to capture excess energy produced by renewable sources, such as, during low-demand times. This saved energy can then be discharged back into the MG when demand increases, which cause to reduce the need for additional grid power and thereby lowering operational costs. By integrating ultracapacitors with traditional batteries, EVs benefit from extended battery life, as ultracapacitors handle high-demand discharges that would then rinsing the battery. This dual-storage method improves the economic efficiency of the MG by minimizing dependency on external energy sources and leveraging saved energy during peak cost periods, ultimately contributing to a more cost-effective and sustainable energy management system.

In Table 6, the cost of the power generation of the generator elements as well as the initiation cost (kWh) is mentioned. The cost of charging and discharging EVs is 0.82 ($/kW). This cost is related to the initial cost, maintenance, parking, etc.

Table 6. Cost of units in MG ($/kW).

	WT($/kW)	PV($/kW)	PAFC($/kW)	EVs/HESS($/kW)
Generation cost	1.073	2.584	0.295	0.82
Startup cost	0	0	1.65	0

After presenting the appropriate pattern of charging and discharging by BC-HBB algorithm, the results are recorded. Fig.8 is related to the cost of the entire network with and without considering the cars. Fig. 8 shows the total electricity cost of the microgrid over a 24-hour period, comparing scenarios with and without the integration of EVs. The integration of EVs leads to notable cost reductions, particularly between 10 and 20 hours, where the cost with EVs consistently falls below the cost without EVs. This discount proves the effectiveness of EVs' V2G abilities, which allow them to supply saved energy back to

the grid during high-demand periods, effectively stabilizing costs and reducing the grid's reliance on more expensive energy sources. For example, around hour 12, the microgrid cost without EVs peaks at approximately $13,525, whereas, with EV integration, this cost is significantly reduced to around $3,874. This difference illustrates the substantial economic impact of using EVs as mobile storage assets that can discharge energy to the grid when electricity prices are high, thereby offsetting peak costs.

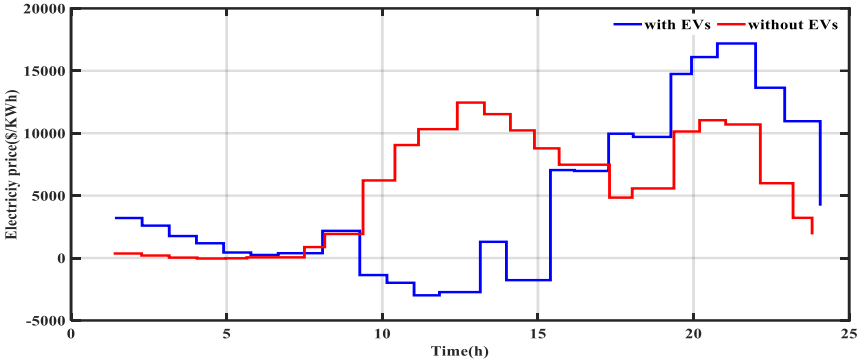

Fig. 8. Energy cost of MG in the absence and presence of Evs.

Overall, the analysis shows that integrating EVs into the microgrid results in a total daily cost reduction of approximately 17.85%. This percentage varies slightly depending on EV usage patterns, grid demand fluctuations, and the timing of V2G participation. By allowing EVs to discharge strategically during peak times, the system not only benefits from cost savings but also achieves greater flexibility and resilience, highlighting the potential of EVs to play a critical role in reducing energy costs and supporting grid stability.

In order to investigate comprehensively the total cost in the end of a day which is shown in Fig .8 is given in Table 7. Also, the obtained cost through the other algorithms is given.

Table 7. Total cost of each Evs.

Total cost	Proposed Algorithm	PSO	GA
Without EVs ($)	132869.9	152730.8	144800.3
With EVs ($)	112981	136875.3	129928.2

In the IEEE 14-bus system, the integration of electric vehicles (EVs) equipped with ultracapacitor batteries has resulted in a significant reduction in total operational costs. Without the presence of EVs, the total cost amounted to 132,869.86$. However, adding the electric vehicles brought the total cost down to 112,981.00$, a cost reduction of almost 15%. This reduction can be attributed to the ability of EVs equipped with supercapacitors to efficiently store and release energy, especially during periods of peak demand. Ultracapacitors provide quick bursts of energy and help balance the grid, reducing reliance on more expensive power generation resources. As a result, the system benefits from improved power management, reduced peak load costs, and improved overall network stability. This proves that electric vehicles and advanced energy storage technology are integrated into the economic and operational benefits of modern energy systems.in Fig.9 the trade power between the upstream grid and IEEE 14 bus system is shown. On the other hand, it is obvious that the obtained result by proposed algorithm in comparison to another algorithm is so better.

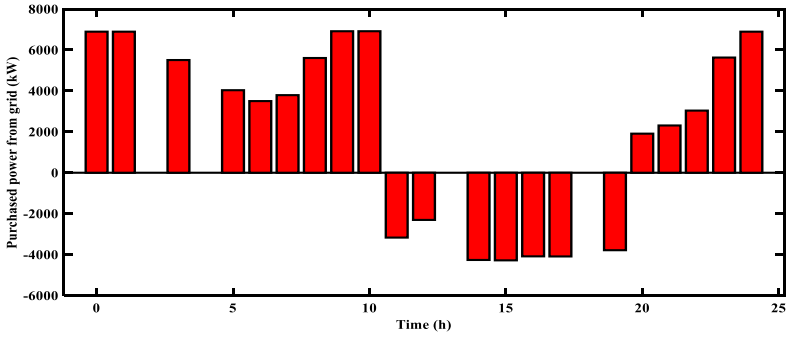

Fig. 9. The exchange power of MG and utility grid.

Based on the provided definition, the main network can inject power into the target network and absorb power from the target network. At hours 1 to 8, due to the low price of electricity, the main network is considered as a power injector. At hours 9 to 14, based on the diagram, the values are negative, indicating that the main network not only did not inject power during these hours, but also absorbed power from the studied network. At hours 15 to 24, the main network is considered as a power injector. Fig.10 represents the power values of each producer per hour.

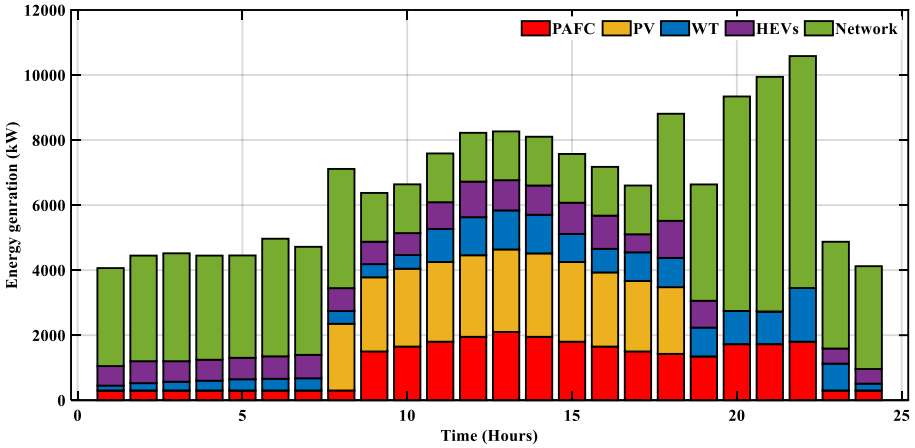

Fig. 10. Amount of produced power of each unit

Based on Fig.10, it can be seen that the integration of ultracapacitors allows EVs to save extra energy, specifically during periods of extra generation from renewable sources such as PV and WT. The ultracapacitor's high energy storage capability enables EVs to arrest and store this excess energy effectively. When there is increased demand in the microgrid, as shown during peak hours, EVs are able to discharge this stored energy back into the microgrid, contributing to overall stability and reducing reliance on the main network supply. This role of ultracapacitors in EVs not only improves energy management flexibility but also optimizes the use of renewable sources, enhancing the efficiency and resilience of the MG system. Also, Fig.10 shows the energy contribution from different sources - PAFC, PV, WT, HEV, grid and battery storage - over a 24-hour period. During peak hours (20:00 to 22:00) the total capacity increases significantly and reaches approximately 10,000 to 12,000 kW. This is fueled by PAFC, WT investment and the recently added Battery Storage providing only 500kW, 550kW at 20:00 21:00, 600 kW 22:00. Throughout the day, PV peaks at 450 kW at 1:00 p.m., while WT peaks at 825 kW around 5:00 p.m. HEVs do not provide power between 20:00 and 22:00 in discharge mode, but the Grid compensates by supplying up to 5000 kW during these peak hours. In general, the distribution of energy ensures the satisfaction of demand, significantly increasing the amount of production during the peak period.

Finally in order to show the superiority of the proposed algorithm, the comparison of proposed algorithm with PSO and GA is shown in Fig.11. A sensitivity analysis is conducted by testing the algorithm with various iteration counts 200, 400, 500, and 700 to determine the optimal balance between convergence and computational efficiency. Fig.11 shows that stable convergence is achieved at 400 iterations for the Big Bang-Big Crunch Hybrid Algorithm, indicated by the flattening of the curve, with minimal further improvement beyond this point. Increasing the iteration count beyond 500 iterations insignificant gains in accuracy while significantly increasing computational time. This finding suggests that 500 iterations provide sufficient performance, ensuring both accuracy and time efficiency. Therefore, 500 iterations are selected as the optimal choice, as they offer reliable results while effectively balancing convergence accuracy and computational resources. Fig.11 compares the convergence of three optimization algorithms HBC-BB hybrid, PSO, and GA over 500 iterations. The BB-BC hybrid algorithm shows superior performance by reaching stability within the first 250 iterations, while PSO and GA take around 350 and 400 iterations, respectively. This faster convergence demonstrates the BB-BC hybrid algorithm's efficiency, making it more suitable for optimization problems that require quick and accurate solutions compared to the slower

convergence of PSO and GA.

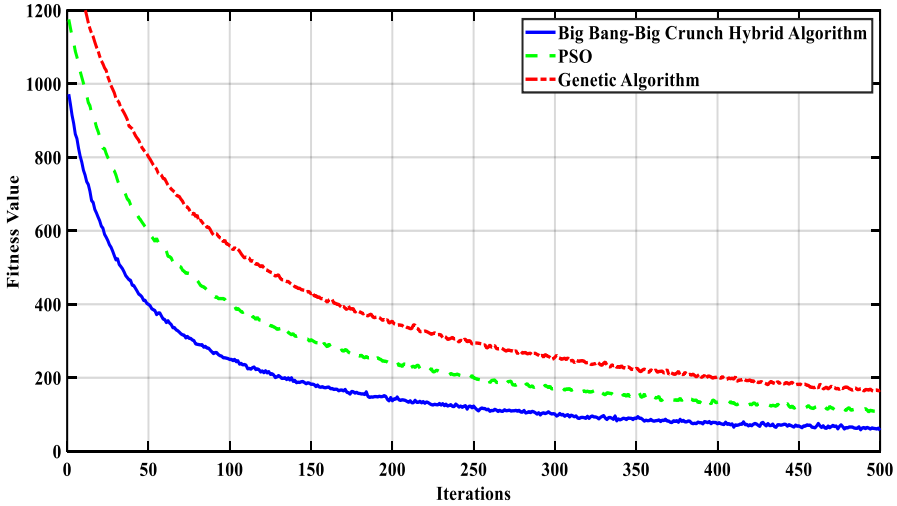

Fig. 11. Comparison between the proposed algorithm and other algorithms.

5. Conclusion

This study introduces a comprehensive energy management approach for the IEEE 14-bus network, including distributed generation and advanced energy storage. The proposed system includes RES (WT, and PV panels), alongside EVs with ultracapacitor batteries, which work as mobile storage, responding rapidly to fluctuations in renewable energy. An intelligent energy management strategy using a hybrid Big Bang-Big Crunch algorithm optimizes EV charging and discharging, coordinating energy flow between generation, storage, and the grid for cost-effective distribution and system stability. By using V2G abilities, EVs help decrease peak loads, and optimal off-peak charging planes further benefit EV owners. Without EV integration, system costs are $132,869.9; with EVs, costs decreased to $112,981, about 15% reduction. The hybrid BB-BC algorithm also compared with PSO and GA, achieving cost reductions of 17% and 13% over these methods, respectively. Although focusing on short-term energy management under ideal conditions, the study is limited in its applicability to scenarios with uncertainties, such as variable EV availability and fluctuating renewables, and usages the small IEEE 14-bus system, restrictive scalability. Future research should integrate long-term strategies, probabilistic models for uncertainties, and expand to larger networks, possibly combining ultracapacitors with batteries or fuel cells, to enhance performance and reliability for real-world applications.

Funding

2024 Jilin Vocational and Technical Education Society, Jilin Vocational Education Research Project (2024XHZ016); Research Project on Teaching Reform of Vocational Education and Adult Education in Jilin Province in 2024 (2024ZCY155).

References

1. Abedinia, O., Lotfi, M., Bagheri, M., Sobhani, B., Shafie-Khah, M., & Catalão, J. P. (2020). Improved EMD-based complex prediction model for wind power forecasting. *IEEE Transactions on Sustainable Energy*, *11*(4), 2790-2802. https://doi.org/10.1109/TSTE.2020.2976038
2. Nurmanova, V., Bagheri, M., Abedinia, O., Sobhani, B., Ghadimi, N., & Naderi, M. S. (2018, October). A synthetic forecast engine for wind power prediction. In *2018 7th international conference on renewable energy research and applications (ICRERA)* (pp. 732-737). IEEE. https://doi.org/10.1109/ICRERA.2018.8567010
3. Shahryari, E., Nooshyar, M., & Sobhani, B. (2019). Combination of neural network and wavelet transform for islanding detection of distributed generation in a small-scale network. *International Journal of Ambient Energy*, *40*(3), 263-273. https://doi.org/10.1080/01430750.2017.1392348

4. Bagheri, M., Nurmanova, V., Abedinia, O., & Naderi, M. S. (2018). Enhancing power quality in microgrids with a new online control strategy for DSTATCOM using reinforcement learning algorithm. *IEEE access*, *6*, 38986-38996. https://doi.org/10.1109/ACCESS.2018.2852941
5. Wang, C., Zhang, Z., Abedinia, O., & Farkoush, S. G. (2021). Modeling and analysis of a microgrid considering the uncertainty in renewable energy resources, energy storage systems and demand management in electrical retail market. *Journal of Energy Storage*, *33*, 102111.
6. Mumtaz, F., Imran, K., Abusorrah, A. and Bukhari, S.B.A., 2023. An extensive overview of islanding detection strategies of active distributed generations in sustainable microgrids. Sustainability, 15(5), p.4456. https://doi.org/10.3390/su15054456
7. Dejamkhooy, A. and Ahmadpour, A., 2022. Prediction and evaluation of electricity price in restructured power systems using Gaussian process time series modeling. Smart Cities, 5(3), pp.889-923. https://doi.org/10.3390/smartcities5030045
8. Nagarajan, K., Rajagopalan, A., Angalaeswari, S., Natrayan, L. and Mammo, W.D., 2022. Combined economic emission dispatch of microgrid with the incorporation of renewable energy sources using improved mayfly optimization algorithm. *Computational Intelligence and Neuroscience*, *2022*. https://doi.org/10.1155/2022/6461690
9. Mokaramian, E., Shayeghi, H., Sedaghati, F., Safari, A. and Alhelou, H.H., 2021. A CVaR-Robust-based multi-objective optimization model for energy hub considering uncertainty and E-fuel energy storage in energy and reserve markets. *IEEE Access*, *9*, pp.109447-109464. https://doi.org/10.1109/ACCESS.2021.3100336
10. Ahmadpour, A., Mokaramian, E. and Anderson, S., 2021. The effects of the renewable energies penetration on the surplus welfare under energy policy. Renewable Energy, 164, pp.1171-1182. https://doi.org/10.1016/j.renene.2020.10.140
11. Hai, T., Zhou, J. and Latifi, M., 2023. Stochastic energy scheduling in microgrid with real-time and day-ahead markets in the presence of renewable energy resources. *Soft Computing*, *27*(22), pp.16881-16896. https://doi.org/10.1007/s00500-023-09021-y
12. Rasoulinezhad, H., Abapour, M., Sadeghian, O. and Zare, K., 2023. The role of risk-based demand response in resource management of a grid-connected renewable-based large-scale microgrid with stationary and mobile energy storage systems and emission tax. *Computers & Industrial Engineering*, *183*, p.109555.
13. Abou El-Ela, A.A., El-Sehiemy, R.A., Allam, S.M., Shaheen, A.M., Nagem, N.A. and Sharaf, A.M., 2022. Renewable Energy Micro-Grid Interfacing: Economic and Environmental Issues. *Electronics*, *11*(5), p.815. https://doi.org/10.3390/electronics11050815
14. Mac Kinnon, M., Razeghi, G. and Samuelsen, S., 2021. The role of fuel cells in port microgrids to support sustainable goods movement. *Renewable and Sustainable Energy Reviews*, *147*, p.111226.
15. Riaz, M., Ahmad, S. and Naeem, M., 2023. Joint energy management and trading among renewable integrated microgrids for combined cooling, heating, and power systems. *Journal of Building Engineering*, *75*, p.106921.
16. Zhou, Y., Wang, J., Wei, C. and Li, Y., 2024. A novel two-stage multi-objective dispatch model for a distributed hybrid CCHP system considering source-load fluctuations mitigation. *Energy*, *300*, p.131557.
17. Ngouleu, C.A.W., Koholé, Y.W., Fohagui, F.C.V. and Tchuen, G., 2023. Optimal sizing and techno-enviro-economic evaluation of a hybrid photovoltaic/wind/diesel system with battery and fuel cell storage devices under different climatic conditions in Cameroon. Journal of Cleaner Production, 423, p.138753.
18. Belkhier, Y., Oubelaid, A. and Shaw, R.N., 2024. Hybrid power management and control of fuel cells-battery energy storage system in hybrid electric vehicle under three different modes. Energy Storage, 6(1), p.e511. https://doi.org/10.1002/est2.556
19. El Mezdi, K., El Magri, A. and Bahatti, L., 2024. Advanced control and energy management algorithm for a multi-source microgrid incorporating renewable energy and electric vehicle integration. Results in Engineering, 23, p.102642.
20. Kostopoulos, E.D., Spyropoulos, G.C. and Kaldellis, J.K., 2020. Real-world study for the optimal charging of electric vehicles. Energy Reports, 6, pp.418-426. https://doi.org/10.1016/j.egyr.2019.12.008
21. Mokaramian, E., Shayeghi, H., Sedaghati, F., Safari, A. and Alhelou, H.H., 2022. An Optimal Energy Hub Management Integrated EVs and RES Based on Three-Stage Model Considering Various Uncertainties. *IEEE Access*, *10*, pp.17349-17365. https://doi.org/10.1109/ACCESS.2022.3146447
22. Dejamkhooy, A. and Ahmadpour, A., 2023. Torque ripple reduction of the position sensor-less switched reluctance motors applied in the electrical vehicles. *Journal of Operation and Automation in Power Engineering*, *11*(4), pp.258-267.

23. O'Neill, D., Yildiz, B. and Bilbao, J.I., 2022. An assessment of electric vehicles and vehicle to grid operations for residential microgrids. *Energy Reports*, *8*, pp.4104-4116. https://doi.org/10.1016/j.egyr.2022.02.302
24. Mokaramian, E., Shayeghi, H., Sedaghati, F., Safari, A. and Alhelou, H.H., 2021. A CVaR-Robust-based multi-objective optimization model for energy hub considering uncertainty and E-fuel energy storage in energy and reserve markets. *IEEE Access*, *9*, pp.109447-109464. https://doi.org/10.1109/ACCESS.2021.3100336
25. Han, Y., Lv, G. and Mokaramian, E., 2020. A review modeling of optimal location and sizing integrated M–FACTS with wind farm and fuel cell. *Journal of cleaner production*, *268*, p.121726.
26. Dejamkhooy, A. and Ahmadpour, A., 2021. Optimal UC and economic dispatching with various small energy resources in the micro-grid using IPPOA and IMILP. Energy Reports, 7, pp.7572-7590. https://doi.org/10.1016/j.egyr.2021.10.124
27. Babanezhad, H. and Ghafouri, A., 2022. Increasing the Accessibility of Rural Microgrid's Load to Resources in Multi-Microgrid System with Considering Minimum Operation Cost. *IEEJ Transactions on Electrical and Electronic Engineering*. https://doi.org/10.1002/tee.23588
28. Natarajan, R., Mehbodniya, A., Ganapathy, M., Neware, R., Pahuja, S., Vives, L. and Asha, 2022. Hybrid big bang–big crunch with ant colony optimization for email spam detection. *International Journal of Modern Physics C*, *33*(04), p.2250051. https://doi.org/10.1142/S0129183122500516